Structure–Property Correlations of Heat-Shrinkable Polymer Blends Based on Ethylene Vinyl Acetate/Carboxylated Nitrile Rubber in the Presence of Different Curatives

S. Ray Chowdhury, C. K. Das

Materials Science Centre, Indian Institute of Technology, Kharagpur 721302, India

Received 26 October 2001; accepted 9 May 2002

ABSTRACT: Elastic memory was introduced into heat-shrinkable polymer blends in the form of an elastomeric phase and through subsequent crosslinking. Blends of ethylene vinyl acetate and carboxylated nitrile rubber with different curative systems were studied with respect to their shrinkability. With an increase in the cure time (the crosslinking density, or memory point), shrinkage increased for the blends with all the curative systems except dicumyl peroxide (DCP). Increasing the elastomer content increased shrinkability because of the increasing driving retraction force of the oriented elastomer phase. A sample stretched at a high temperature (HT) showed greater shrinkage than a sample stretched at room temperature (RT) because of the greater concentration and degree of orientation of the extended chains. Generally, the crystallinity of the stretched (RT and HT) samples was higher than that of ordinary unstretched and shrunk samples, and this increased the effectiveness of intermolecular interactions in the former. For all systems except DCP, RT-stretched samples showed higher crystallinity than corresponding HT-stretched samples. With RT stretching, rapid extension and subsequent recrystallization occurred in samples molten at high local values of the stored elastic energy. An increase in the crosslinking density and orientation of the blends increased the thermal stability because of the formation of strong networks and compact structures. © 2002 Wiley Periodicals, Inc. J Appl Polym Sci 87: 1414–1420, 2003

Key words: elastomers; polyolefins; thermal properties; X-ray

INTRODUCTION

Several properties can be improved by the melt blending of thermoplastic materials and elastomers, with some of the other properties maintained. For the design of new polymeric materials, a knowledge of structure–property relationships is required. Chain orientation in effect provides a means of tailoring and improving the properties of polymers.[1] The heating and subsequent shrinking of these oriented materials can result in useful properties. Applications include heat-shrinkable and flame-retardant polypropylene tubes, cables, heat-shrinkable furniture webbing, pipe filling, medical devices, and encapsulation.[1]

The total linear deformation of an orientated sample may be described by three rheological components:[2]

1. An instantaneous elastic component, E_1, caused by bond deformation or bond stretching, which is completely recoverable when the stress is released (Hookian behavior).
2. A viscoelastic component, E_2, caused by uncoiling, which is frozen in the structure when cooled.
3. A plastic (viscous) component, E_3, caused by molecules slipping over one another, which is nonrecoverable. E_2 can serve as a measure of the degree of recoverable orientation, which is linked to the thermoelastic shrinkage.[3]

In fact, the heat shrinkability, a collective property, is affected by highly oriented amorphous materials,[4] crystalline regions,[5] the average orientation of the molecular chain axes in crystals approaching a microfibrillar state,[5] and memory points (crosslinks).[6,7] Stretching at a high temperature (HT) reduces dimensional stability because the molecules have been stretched into a statistically improbable conformation of thermodynamically high energy and low entropy.[8] This results in positive free energy, that is, far from thermodynamic equilibrium. The stretched state, which represents a frozen-in morphology, provides a driving force that causes the materials to snap back to a more stable (lower energy and higher entropy), randomly coiled conformation,[9] resulting in a macroscopic recovery to the dimensions of the original state.

In this study, elastic memory was introduced into the system in the form of an elastomer phase. The elastomer phase or the elastomer and plastic phases

Correspondence to: C. K. Das (ckd@matsc.iitkgp.ernet.in).
Contract grant sponsor: CSIR.

were cured, and this could change the microstructure of the blends. Therefore, structure-related properties, especially shrinkability, could be affected. Consequently, shrinkability was studied for blends of elastomers [carboxylated nitrile rubber (XNBR)] and plastics [ethylene vinyl acetate (EVA)] in the presence of different curative systems. For the observation of the structures and structure-dependent properties of the polymer blends, X-ray diffraction analysis was considered as an essential tool, providing much useful information concerning the internal arrangement of the molecules in the polymers. Through a thermal study, variations in the thermal stability, heat of fusion (ΔH_f), and heat of oxidative degradation (ΔH_o) were investigated satisfactorily.

Recently, Das and coworkers[10–13] studied the flame retardancy and heat shrinkability of polyolefin/elastomer blends and EVA/elastomer blends. This investigation aims to establish a correlation between shrinkability and some structure-dependent properties in blends of XNBR and EVA in the presence of different curative systems.

EXPERIMENTAL

Materials

The thermoplastic used was Pilene EVA-1802, which was supplied by Polyolefins Industries, Ltd. (Mumbai, India). The vinyl acetate content was 18 wt %, the density was 0.937 g/cc, and the melt flow index was 2.0 g/10 min.

The XNBR used was Nipol N-34 from Nippon Zeon Co., Ltd. (Tokyo, Japan); the density was 0.98 g/cc, the Mooney viscosity was 45 at 100°C, and the bound acrylonitrile content was 27%. The compounding formulations are given in Table I.

TABLE I
Compounding Formulation

Sample	XNBR (g)	EVA (g)	S/MBT/MBTS (phr)	MDA/DPG (phr)	DCP (phr)
1(a)	10	90	—	—	—
1(b)	30	70	—	—	—
1(c)	50	50	—	—	—
1(d)	70	30	—	—	—
2(a)	10	90	1.5/2.0/2.0	—	—
2(b)	30	70	1.5/2.0/2.0	—	—
2(c)	50	50	1.5/2.0/2.0	—	—
2(d)	70	30	1.5/2.0/2.0	—	—
3(a)	10	90	—	1.0/1.0	—
3(b)	30	70	—	1.0/1.0	—
3(c)	50	50	—	1.0/1.0	—
3(d)	70	30	—	1.0/1.0	—
4(a)	10	90	—	—	1.0
4(b)	30	70	—	—	1.0
4(c)	50	50	—	—	1.0
4(d)	70	30	—	—	1.0

For samples 2 and 3, phr are based on elastomer phase, and for sample 4, phr are based on both the phases. S = sulfur; MBT = 2-mercaptobenzothiazole; MBTS = 2-mercaptobenzothiazole disulfide; MDA = 4,4′-diaminodiphynylmethane; DPG = diphenyl guanidine.

Preparation of the blends

The EVA/XNBR blends were prepared with different compositions and different curative systems, as shown in Table I, in a Brabender plasticorder for 10 min at 30 rpm. The mixing temperature was 100°C. EVA was first put into the mixing chamber and allowed to melt at a low shear rate. XNBR was then added slowly. After the complete addition of XNBR, the curatives (Table I) were added sequentially. The blending was allowed to continue for 8 min, after which the blends were taken out and sheeted in an open two-roll mixing mill. The blends, in sheet form, were compression-molded at 150°C for 10, 20, 30, 40, or 50 min. The specimens cut from the molded slabs were used for the shrinkage measurements, and these were used for conducting the technical studies.

Measurements of shrinkage

The orientation was obtained with two different methods: (1) hot drawing above the melting point (T_m) followed by quenching in air and (2) cold stretching ($T_g < T_{def} < T_m$, where T_g is the glass-transition temperature) between T_g and T_m. In the latter case, deformation occurred in the solid state, in which changes in the shapes and alignments of the crystallites led to orientation.[9]

The lengthwise shrinkage was measured at two different temperatures:

1. Vulcanizates were stretched at ambient temperature [room temperature (RT)], that is, below T_m. The shrinkage was measured at 150°C.
2. Vulcanizates were stretched at 150°C (HT), and the shrinkage was measured at the same temperature.

The shrinkage (S_h) was measured as follows:

$$S_h\,(\%) = (L_{str} - L_s)/(L_{str}) \times 100$$

where L_{str} is the length of the sample after stretching and L_s is the length of the sample after shrinking. The draw ratio was 5 (length of the stretched sample/length of the usual unstretched sample). The drawing rate was 360 mm/min.

Thermal analysis

Thermogravimetric analysis (TGA) and differential scanning calorimetry (DSC) studies were carried out

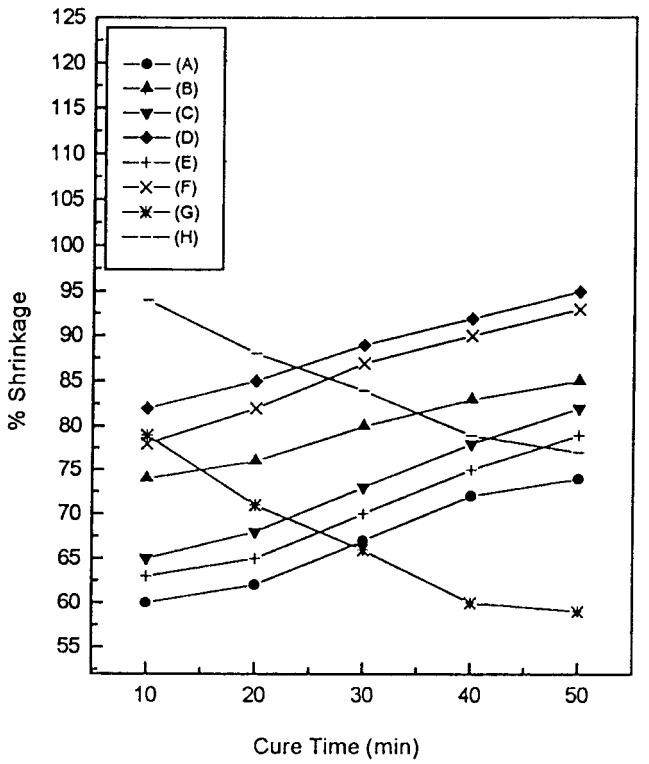

Figure 1 Variation of the shrinkage percentage with the cure time at a constant elastomer content of 30%: (A) 1(b), RT-stretched sample; (B) 1(b), HT-stretched sample; (C) 2(b), RT-stretched sample; (D) 2(b), HT-stretched sample; (E) 3(b), RT-stretched sample; (F) 3(b), HT-stretched sample; (G) 4(b), RT-stretched sample; and (H) 4(b), HT-stretched sample.

with a Stanton Redcroft STA-625 thermal analyzer from 25 to 580°C at a heating rate 10°C/min in air.

Cure characteristics

The cure characteristics of the blends were studied with a Monsanto R-100 rheometer at 150°C for 60 min.

RESULTS AND DISCUSSION

Effects of the cure time and elastomer content on the shrinkability of the blends

The variations of the shrinkage with the cure time (i.e., the thermal activation time; the duration for which the material was compression-molded at HT was considered the cure time for a noncurative system) of the EVA/XNBR blends with different curative systems are shown in Figure 1. With an increase in the cure time, the shrinkability increased for all cases (although to different extents), except for samples 4(a–d), at both temperatures of stretching (ambient temperature and 150°C). Because the crosslinks behaved as memory points in the stretched sample, the recovery was higher; that is, higher shrinkage was obtained with an increase in the cure time for a particular blend because of the increase in the amount of crosslinking (shown later in Fig. 5). For samples 4(a–d) (Table I), a longer cure time produced a greater number of crosslinks in both phases. The extensibility of the blend decreased because the plastic phase, which was crosslinked, controlled the extensibility. Consequently, the contribution of the orientation of the amorphous phase to the shrinkability decreased, bringing down the recovery, that is, the shrinkage.

Figure 2 shows that with an increasing elastomer content, the shrinkage increased at a fixed cure time. An opposite trend was observed beyond a 50% elastomer content for samples 4(a–d). The polymer chains in the stretched conditions exited in four states, and they could be classified as crystalline and amorphous states of coiled and extended chains.[14,15] Only the extended state (the average orientation of the molecular chain axes in the crystal and noncrystalline regions) could provide a driving force for the contraction of the stretched samples.[16,17] The major part of the driving retraction force was provided by comparatively highly oriented amorphous materials. In addition, memory points that depended on the amount of crosslinking[13] increased the shape memory effect, that is, the shrinkability. Therefore, elastomer-rich blends

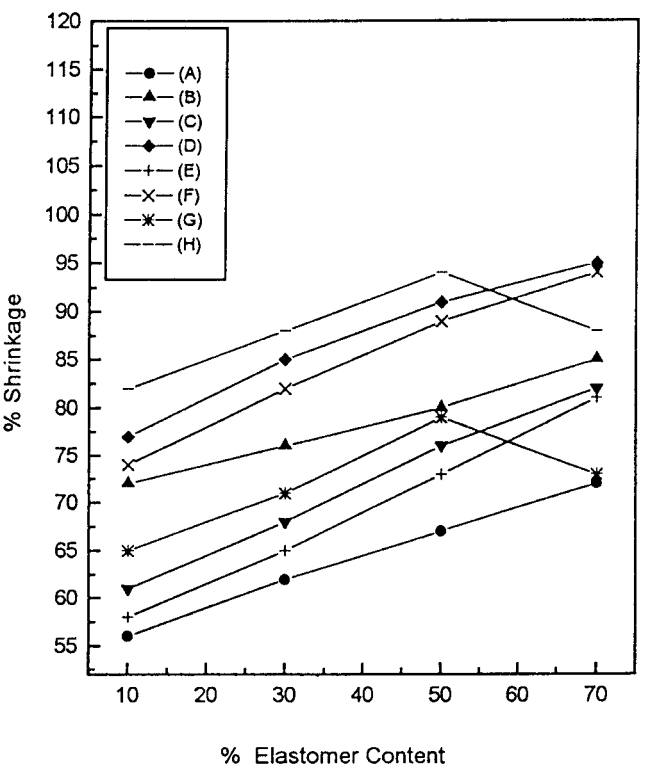

Figure 2 Variation of the shrinkage percentage with the elastomer content at a constant cure time of 20 min: (A) 1, RT-stretched sample; (B) 1, HT-stretched sample; (C) 2, RT-stretched sample; (D) 2, HT-stretched sample; (E) 3, RT-stretched sample; (F) 3, HT-stretched sample; (G) 4, RT-stretched sample; and (H) 4, HT-stretched sample.

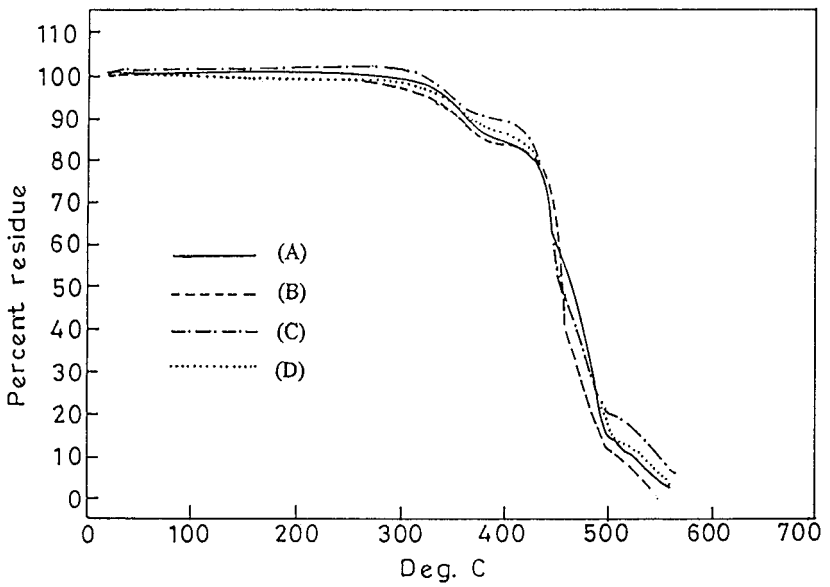

Figure 3 TGA plots: (A) 4(b), usual unstretched sample; (B) 4(b), RT-stretched sample; (C) 4(b), HT-stretched sample; and (D) 4(b), HT-shrunk sample.

had a tendency to revert to a randomly coiled, thermodynamically favorable conformation, increasing the shrinkage. Again, an increase in XNBR meant an increase in memory points (where only the elastomer phase was crosslinked), which produced higher shrinkage. From Figures 1 and 2, it is obvious that the shrinkability of samples 2 and 3 was more sensitive toward the elastomer content as the extent of crosslinking (only in the elastomer phase) was higher in these samples in comparison with the other two (shown later in Fig. 5). However, the shrinkability of sample 4 was most sensitive, although in the opposite direction, toward the cure time, and that of sample 1 was the least sensitive toward the cure time. The highest torque value was found in the dicumyl peroxide (DCP) system (sample 4), and no rise in the torque was found in the noncurative system (sample 1). For sample 4, beyond a 50% elastomer loading, probably because of the lower amount of the plastic, which was again crosslinked, the extensibility of the blend decreased remarkably, lowering the shrinkability, unlike the others. It is obvious from Figures 1 and 2 that the HT-stretched samples showed higher shrinkage than the RT-stretched samples for all the systems. Two factors, according to Capaccio and Ward,[18] are involved in the shrinkage of RT-stretched ($<T_m$) samples. One is the contraction of the amorphous chain, and the other is the reorganization of the crystalline phase, in which deformation occurs in the crystals and the lamellae of the crystals can slip and orient, approaching a microfibrillar structure.[5] If the crystal deformation is less, then the contribution of the second factor will be less for the recovery, and the first factor will only control the shrinkage. For an RT-stretched sample, the second factor is mainly responsible for shrinking. However, for an HT-stretched sample, there is no crystalline structure, as the sample is in the molten state, so the first factor is important. An HT-stretched sample shows higher shrinkage because of the greater concentration and extent of orientation of the extended chains.

Thermal analysis

HT TGA and DSC plots of various blends with various curative systems are displayed in Figures 3 and 4, respectively. The results of TGA and DSC are summarized in Table II. Every sample underwent two steps of degradation, although the degradation began at different temperatures. It is clear from Table II that the trend of the changes in the initial degradation temperature (T_1) is a reflection of the efficiency of the curing agents (Fig. 5). It is also evident that the stretched samples were thermally more stable than the corresponding unstretched samples. This may be due to the stability and continuity of the skeleton in the orientation axis offered by orientation. The shrunk samples began their initial degradation earlier than the usual unstretched samples. The variations of the second degradation temperature (T_2) follow the trend of T_1, with respect to the crosslinking agents and processing (stretching and shrinking). With the crosslinking efficiency, the 50% decomposition temperature (T_{50}) and 90% decomposition temperature (T_{90}) also follow the trend of T_1 and T_2. With stretching and subsequent shrinking, the T_{90} values are almost in line with those of T_1 and T_2. However, the T_{50} values were reduced with stretching and went down more

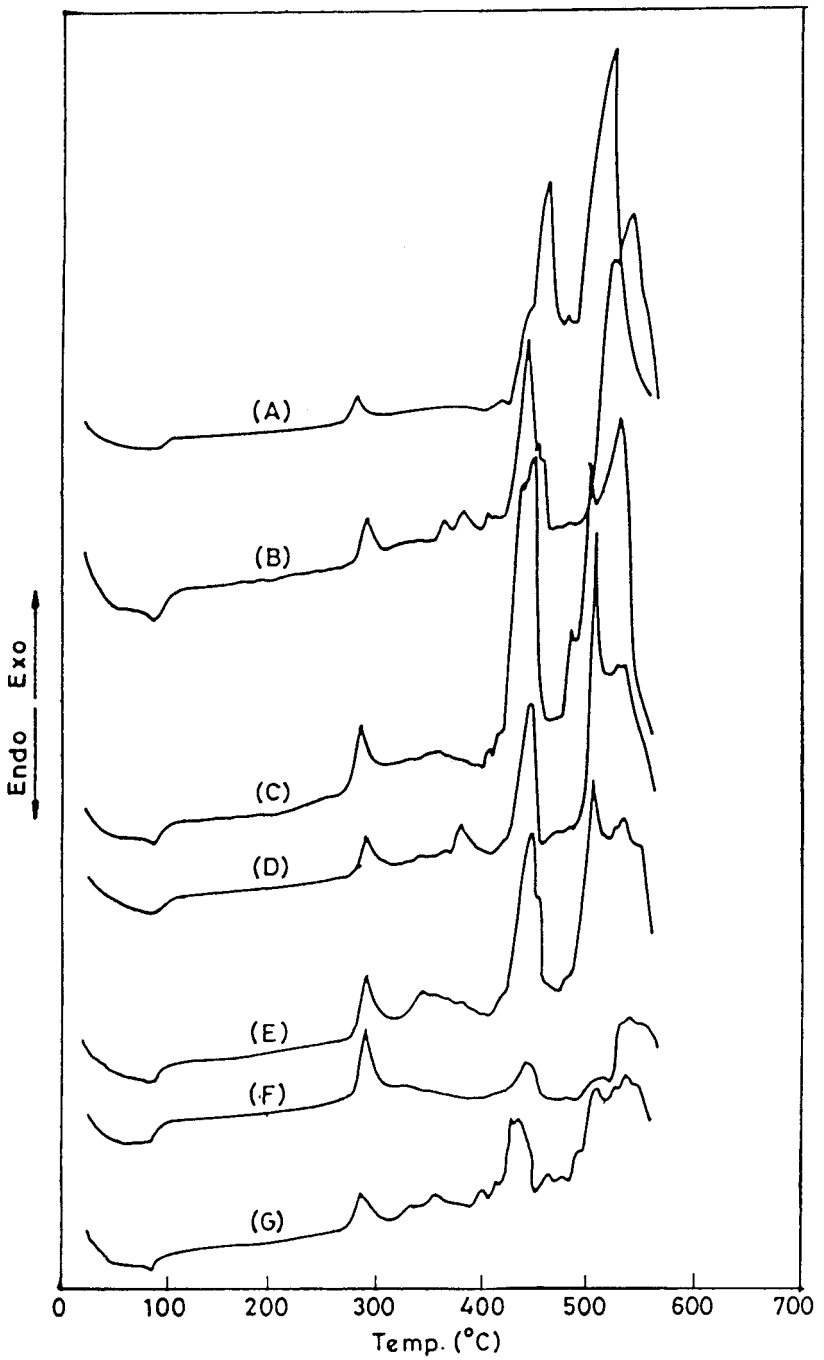

Figure 4 DSC plots: (A) 1(b), usual unstretched sample; (B) 2(b), usual unstretched sample; (C) 3(b), usual unstretched sample; (D) 4(b), usual unstretched sample; (E) 4(b), RT-stretched sample; (F) 4(b), HT-stretched sample; and (G) 4(b), HT-shrunk sample.

with shrinking. More experimentation is required to explain this finding. In DSC, the T_m values were almost unchanged, regardless of the curing agents and HT processing. In this respect, one thing to be noticed is that crystals melt at a temperature below their thermodynamic equilibrium melting temperature because of an excess of free energy of the crystalline and amorphous phases, and this might be the cause of the slight variations of T_m listed in Table II.

The recovery properties of the stretched samples depended strongly on the crystalline structure.[15] The oriented chains in the amorphous phase of the stretched samples (cooled down to RT) were internally stressed and restricted to relax by crystallization.[16] With heating to T_m or higher, stretched samples without external constraints relaxed to an isotropic state, and this resulted in a macroscopic recovery to the dimensions of the original state.[18,19] As with an increase in crystallization, the internal

TABLE II
TGA/DSC Results

Sample	T_m (°C)	T_1 (°C)	T_2 (°C)	T_{50} (°C)	T_{90} (°C)	ΔH_f(mcal/mg)	ΔH_o(mcal/mg)
1(b) [usual]	87	310	427	447	510	18	733
2(b) [usual]	86	320	437	457	513	28	378
3(b) [usual]	89	313	433	450	510	23	476
4(b) [usual]	86	333	440	466	526	41	336
4(b) [RT-stretched]	85	338	445	450	533	42	231
4(b) [HT-stretched]	86	342	447	456	550	41	110
4(b) [HT-shrunk]	88	314	430	447	520	42	315

stress was increased, so the degree of disorientation was high. The shrinkage values of different samples with different curative systems were in good agreement with ΔH_f, a measurement of crystallinity, although some discrepancies were observed for sample 4(b).

With processing (stretching and shrinking), sample 4(b) did not change with respect to its ΔH_f values. The crosslinks in the plastic phase, unlike others, probably led to this new occurrence. The highest and lowest ΔH_o values were found for samples 1(b) and 4(b), respectively. These results conformed with the extent of crosslinking. The oxidation of the polymer occurred in the amorphous region because the crystallites were impermeable to oxygen,[20] and the rate of the chemical initiating step was dominated by the physical accessibility of the polymer structure.[21] Furthermore, the ΔH_o value was reduced by stretching, and that of the HT-stretched sample was lower than that of the RT-stretched sample. This happened because of the close packing and the increase in the effectiveness of the intermolecular interactions offered by the extent of orientation. However, the ΔH_o value of an HT-shrunk sample was lower than the value of a usual unstretched sample. The probable area to be attacked by oxygen was reduced in the shrunk sample because of an increase in the free zone through recoiling, and this reduced ΔH_o.

CONCLUSIONS

The shrinkage property of the EVA/XNBR blends depended on the cure time, the elastomer content, the temperature, and the nature of the crosslinking agent. Therefore, the shrinkability could be controlled through control over the time, elastomer ratio, temperature, and crosslinking agents. Highly crosslinked and HT-stretched blends showed higher shrinkage than low crosslinked and RT-stretched samples, respectively, for EVA/XNBR systems. The blends in which both phases were crosslinked [4(a–d)] showed different shrinkage properties: at the lower range of the cure time, there was higher shrinkage, but at higher cure times, there was lower shrinkage. The shrinkage was associated with the crystallinity (ΔH_f), which depended on the curing agent, crosslinking

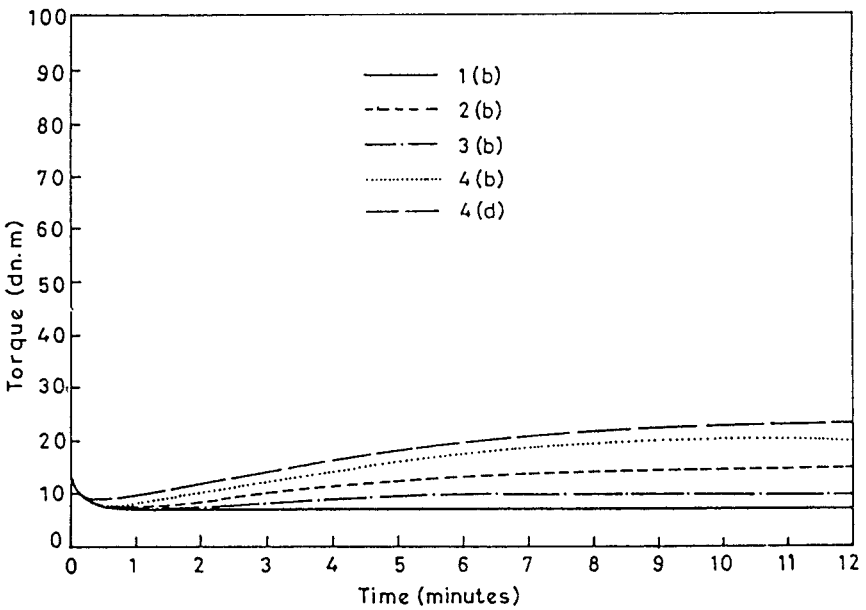

Figure 5 Variation of the rheometric torque with the cure time.

efficiency, and so forth. HT processing, the efficiency of the curatives, and the extent of crosslinking played important roles concerning the thermal stability. A greater amount of crosslinks and greater orientation affected the thermal stability.

References

1. Rosato, D. V. Roato's Plastic Encyclopedia and Dictionary; Hanser: Munich, 1993; p 508.
2. Karam, J.; Williams, J. L. Mod Plast 1953, 30, 119.
3. Ohma, J.; Monson, L.; Sperling, H. Polym Blends Compos 1981, 5, 69.
4. Dechndia, F.; Russo, R.; Vittoria, V. J Polym Sci Polym Phys Ed 1982, 20, 1175.
5. Samuels, R. J. Science and Technology of Polymer Films; Wiley-Interscience: New York, 1968; Chapter 7.
6. Patra, P. K.; Das, C. K. J Appl Polym Sci 1998, 68, 597.
7. Ray Chowdhury, S.; Das, C. K. J Appl Polym Sci 2000, 77, 2088.
8. Geil, P. H.; Baer, E.; Wada, Y. The Solid State of Polymers; Marcel Dekker: New York, 1974.
9. Encyclopedia of Polymer Science and Engineering, 2nd ed.; Mark, H. F.; Bikales, N. M.; Overberger, C. G.; Menges, G.; Kroschwitz, J. I., Eds.; Wiley-Interscience: New York, 1987; Vol. 7.
10. Ray Chowdhury, S.; Das, C. K. J Appl Polym Sci 2000, 77, 2088.
11. Ray Chowdhury, S.; Das, C. K. Polym Adv Technol 2000, 11, 359.
12. Ray Chowdhury, S.; Das, C. K. Polym Polym Compos 2000, 8, 177.
13. Patra, P. K.; Das, C. K. J Polym Eng 1997, 17, 231.
14. Luo, X. L.; Zhang, X. Y.; Wang, M. T.; Ma, D. Z. J Appl Polym Sci 1997, 64, 2433.
15. Wang, M.; Zhang, L. J Polym Sci Part B: Polym Phys 1999, 37, 101.
16. Pakula, T.; Trznadel, M. Polymer 1985, 26, 1011.
17. Samuels, R. J. J Polym Sci Polym Phys Ed 1972, 10, 781.
18. Capaccio, G.; Ward, I. M. Colloid Polym Sci 1982, 46, 260.
19. Sarvaranta, L. J Appl Polym Sci 1995, 56, 1085.
20. Billingham, N. C. Atmospheric Oxidation and Antioxidants, 2nd ed.; Elsevier: New York, 1993; Vol. 2, Chapter 4.
21. Scott, G.; Gilead, D. Degradable Polymer; Chapman & Hall: London, 1995.